Clay Minerals, (2018) **53**, 29–39

Application of polyether amine, poly alcohol or KCl to maintain the stability of shales containing Na-smectite and Ca-smectite

SHIFENG ZHANG[1,*], YANFENG HE[1], ZHIXUE CHEN[2], JAMES J. SHENG[3] AND LIPEI FU[1]

[1] *Department of Petroleum Engineering, Changzhou University, China*
[2] *CNPC Drilling Research Institute, Beijing, China*
[3] *Department of Petroleum Engineering, Texas Tech University, USA*

(*Received 22 July 2017; revised 29 January 2018; Associate Editor: Balwant Singh*)

ABSTRACT: The stability of a shale containing smectite with different exchangeable cations (Na^+, Ca^{2+}) was improved using optimum solutions containing polyether amine (PA), poly-alcohol (PO) or KCl. Two types of shale samples with Na^+ and Ca^{2+} as the main exchangeable cations, respectively, were used and the optimized solutions were determined using X-ray diffraction (XRD), an adsorption test, an oedometer swelling test, and an immersion test. The use of KCl prevented intercalation of PA or PO and maintained the stability of the Na-smectite-bearing shale. PA or PO adsorption reduced water adsorption sites on the clay layer, and K^+ reduced hydration of exchangeable Na^+, resulting in good shale stability in mixed solutions of KCl+PA, and KCl+PO. More stable shale was achieved in KCl^+ PA mixed solution, whereas in the KCl^+ PO solution the transport of water or solute molecules in the shale was reduced. In the shale containing mainly Ca-smectite, PA, PO and KCl maintained shale stability when applied separately or in common, as PA or PO cannot exchange Ca^{2+} in the smectite interlayer. As a result, PA or PO should be used together with KCl during drilling in shale formations containing Na-smectite, whereas in shales with Ca-smectite, PA, PO or KCl may be used separately.

KEYWORDS: shale stability, Na^-, Ca-smectite, shale inhibitors, hydration swelling.

During drilling operations, shale hydration and the resulting well-bore instability problems, including hole collapses, tight holes, stuck pipes, poor hole cleaning, hole enlargement and plastic flow, may lead to the loss of US$ billions per year, worldwide (Zeynali, 2012; Zhang *et al.*, 2016). Water adsorption on cations and swelling clay minerals in shales are the main cause, as they may contribute to swelling of the rock and may cause severe structural damage and fracturing (Heidug & Wong, 1996; Zhang *et al.*, 2016).

*E-mail: cczuzhang87@163.com
https://doi.org/10.1180/clm.2018.2

Smectite is a well-known contributing factor to the majority of the reported stability problems, due to its large surface area, negative surface charge, and ability to swell in the presence of water (Mao *et al.,* 2010). Na^+ and Ca^{2+} are among the most common interlayer cations of smectite. In Na-smectite, two- and three-layer cation hydrates may form with the bilayer water adsorption on the external surface at high water-vapour pressure (Cases *et al.*, 1992). The osmotic swelling of the smectite from the two-layer hydration state is an isoenthalpic process. The hydration of Na^+ is the main contribution to the overall hydration of Na-smectite (Salles *et al.*, 2007). In Ca-smectite, the two-layer hydrate forms at high water-vapour pressure (Cases *et al.*, 1997).

Among the compounds used to reduce shale hydration (Burchill *et al.*, 1983; Caenn and Chillingar, 1996; Nelson and Cosgrove, 2005; Rosa *et al.*, 2005; Souza *et al.*, 2010), potassium chloride and poly alcohol are the conventionally used agents; the use of polyether amine compounds with small molecular masses are a recent advance (Qu *et al.*, 2009; Cui and Van Jeroen, 2010; Wang *et al.*, 2011; Zhong *et al.*, 2011; Zhang *et al.*, 2015, 2016). To determine the optimal solutions, two shale samples with different exchangeable cations (Na^+ and Ca^{2+}) were studied, by means of K^+, PO and PA adsorption isotherms tests, analysis of shale and shale composites XRD, oedometer swelling tests, and by examination of imaging of the shale core after immersion.

EXPERIMENTAL

Shale characterization

The mineralogical composition of the shale sample was determined by XRD using an X'Pert-Pro MPD diffractometer (PANalytical B.V.; Netherlands) with Cu-*K*α radiation, equipped with a solid-state detector, operating at 40 kV and 40 mA, according to SY/T 5163 (1995), SY/T 5983 (1995) and SY/T 6210 (1996). The exchangeable cations in the shale were replaced by Ba^{2+} (Jiang & Zhang, 2005) and the ion species and content were measured using an Agilent ICP-720ES inductively coupled plasma atomic emission spectrometer (ICP-720ES, Agilent Technologies Corporation, USA).

Quartz is the dominant phase, with the total clay fraction being 36% and 21% in the H and T shale samples, respectively (Table 1). Illite and mixed-layer illite-smectite (I-S) clay are the main clay phases in both shale samples with chlorite and kaolinite being minor phases. The total exchangeable cations content is 20.20 and 2.89 mmol/100 g shale, for the H and the T shales, respectively. Na^+ is the main exchangeable cation in H shale while Ca^{2+} is the exchangeable cation in T shale. It is inferred that the H shale contains abundant Na-smectite while T shale contains mainly Ca-smectite.

The shale samples were ground, sieved, washed and dispersed in water to form 40 g/L aqueous suspensions. The solid content was measured after drying at 100°C until constant weight was achieved.

Chemicals

The PA used in this study was developed by the drilling fluid research team at the China University of Petroleum (Zhong *et al.*, 2011; Zhang *et al.*, 2016). The PA molar mass was ~400 g/mol and its typical chemical formula was CH_3-$[OCH_2CH_2]_x$-$[OCH_2(CH_3)CH]_y$-NH_2. PO has a typical formula HO-$[OCH_2CH_2]_x$-. $[OCH_2\ (CH_3)\ CH]_y$-OH, was provided by Shengli Drilling Institute of Sinopec Corporation, China. The PO molar mass was ~1000 g/mol. Analytically pure KCl was purchased from Sinapharm Chemical Reagent Co. Ltd.

Experimental

Adsorption isotherms of PA, PO, K^+ on shale sample and released ion measurement. Aqueous PA, PO and KCl stock aqueous solutions were prepared and mixed with the shale sample stock suspension to form 1wt.% shale suspensions with various concentrations of PA, PO or KCl. The procedure to determine the amount of PA, PO and K^+ adsorbed on shale from solutions of various concentrations and the cations released during adsorption was reported by Zhang *et al.* (2015). The carbon content in the dried shale-PA composite was analysed using a Euro EA3000 elemental analyzer (Euro Vector S.P.A.; Italy). The contents of K^+ and the cations released from the shale to the supernatant was determined by ICP-OES.

XRD analysis. The shale and shale-PA (PO or K^+) composite solutions were centrifuged using a 5000×g centrifugal force for 30 min and washed twice with deionized water. Then they were mounted evenly on glass slides and subsequently placed in desiccators with a saturated K_2SO_4 solution at ~98% relative humidity (RH) for one month. X-ray diffraction analysis was used to determine the d_{001} spacing of smectite in both the shale and shale composite. The same samples were subsequently placed in desiccators with silica gel at ~0% RH for one month and XRD analysis was conducted to record the d_{001} spacing of smectite.

Shale oedometer swelling tests. Swelling tests were carried out in a fixed-ring oedometer, according to ASTM D 4546, Method B (1996). The specimens were allowed to swell when immersed in the PA, PO or KCl solution. The vertical displacement at different times was measured using a digital dial gauge. Digital photographs of the shale were also taken after immersion in the solutions.

https://doi.org/10.1180/clm.2018.2 Published online by Cambridge University Press

TABLE 1. Mineralogical and exchangeable cation composition of H and T shales.

Shale #	Proportion of minerals in total sample (%)								
	Quartz	Potassium feldspar	Plagioclase	Calcite	Ankerite	Siderite	Analcime	Hematite	Total clay
H	28	5	13	7	4	–	5	2	36
T	37	5	18	10	4	2	2	1	21
Shale #	Proportion of clay minerals in total clay (%)								
	Illite	Kaolinite	Chlorite	Mixed-layer (illite-smectite)					
H	28	4	4	64					
T	41	4	18	37					
Shale #	Proportion of layers in mixed-layer illite-smectite (%)								
	Smectite			Illite					
H	20			80					
T	20			80					
	Proportion of exchangeable cations in clay minerals (mmol/100 g shale)								
Total cations contents exchanged	Ca^{2+}	K^+	Mg^{2+}	Mn^{2+}		Na^+		Sr^{2+}	
20.20	1.03	0.14	0.168	0.0022		18.86		0.004	
2.89	2.60	0.022	0.045	0.0052		0.22		0.0008	

RESULTS AND DISCUSSION

PA,K^+ adsorption on H and T shale samples

The H shale absorbed more PA than the T shale (Fig. 1). The rate of adsorption of PA on H shale and that of release of Na^+ cations were high at low PA concentrations, decreasing at high concentrations. Because the T shale is poor in Na^+ ions, only small amounts of PA may adsorb on shale by exchanging Na^+. Moreover, K^+, Ca^{2+} and Mg^{2+} were not detected in solution in either the H or the T shale, indicating that no K^+, Ca^{2+} and Mg^{2+} were exchanged by PA. The main mechanisms for PA adsorption include ion exchange and adsorption on the clay layer (Greenwell *et al.*, 2005; Cui & Van Jeroen, 2010). It is suggested that both ion exchange and clay-layer adsorption contributed to the adsorption of PA on H shale, whereas adsorption on the clay layer was the main mechanism for PA adsorption on T shale.

The rate of adsorption of PO was high at low PO concentrations, reaching a plateau at high PO concentrations in both shales (Fig. 1). The adsorption isotherm showed a monolayer adsorption in the T shale, and multilayer adsorption in the H shale (Zhao, 2005). No cations were exchanged during PO adsorption in either H shale or T shale (Fig. 2). Previous work has shown that PO is adsorbed on smectite mainly through: (1) H-bonding between oxygen atoms of the PEO segments and siloxane groups of the clay surface; (2) H-bonding between oxygen atoms of the PEO segments and water molecules in the hydration shells of the exchangeable cations; and (3) direct coordination or ion-dipole interaction between the oxygen atoms of the PEO segments and the exchangeable cations, with a distorted and extended conformation in the interlayer of smectite, which was an intermediate form of the helical and planar zigzag conformations (de Bussetti & Ferreiro, 2004; Deng *et al.,* 2006). In the T shale, the exchangeable Ca^{2+} may impede separation of the smectite layers (de Bussetti & Ferreiro, 2004), causing monolayer adsorption of PO. In the H shale, separation of the clay layers resulted in multilayer adsorption and larger amounts of adsorbed PO.

When K^+ was adsorbed to the H or T shale samples, all the Na^+ in the shale was exchanged whereas no Ca^{2+} or Mg^{2+} was exchanged by K^+ (Fig. 1).

In mixed solutions, the amount of PA adsorbed on H shale was slightly greater than that adsorbed on shale T (Fig. 1). In the mixed solution, the amount of PA adsorbed on the H shale decreased significantly, whereas the amount of PA adsorbed on the T shale was comparable to the solution containing only PA. All Na^+ was exchanged by K^+ in mixed solution without PA or PO (Fig. 2). With increase in the PA or PO

https://doi.org/10.1180/clm.2018.2 Published online by Cambridge University Press

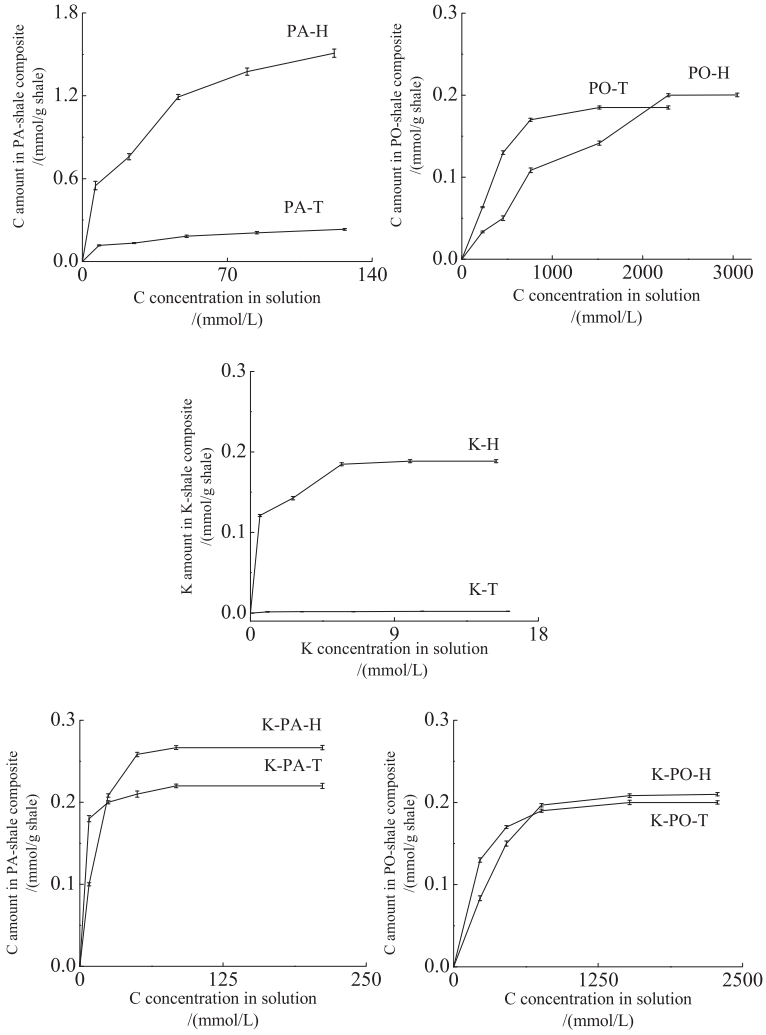

FIG. 1. Adsorption of PA on H and T shale (PA-H, PA-T); adsorption of PO on H and T shale (PO-H, PO-T); adsorption of K^+ on H and T shale (K-H, K-T); adsorption of PA on H or T shale in mixed solution of PA and 1 mol/L KCl (K-PA-H, K-PA-T); adsorption of PO on H or T shale in mixed solution of PO and 1 mol/L KCl (K-PO-H, K-PO-T).

concentration, the amount of exchanged Na^+ in the H and T shale samples remained constant. K^+ adsorption may reduce the amount of exchangeable Na^+ (Zhang *et al.*, 2016). In a mixed solution, PA adsorption by Na^+ exchange on H shale was reduced or prevented, and clay-layer adsorption became the main mechanism for both H and T shale samples. As a result, PA adsorption was greatly reduced on the H shale and was similar to that on the T shale.

In mixed solutions, the amount of PO adsorbed on the H shale was similar to that on the T shale (Fig. 1e). Moreover, the amount of PO adsorbed on the H shale decreased slightly, whereas that adsorbed on the T shale was comparable to that in solution containing only PO. In shale H, the adsorption of PO on smectite surfaces from mixed solutions formed a multilayer, which changed to monolayer in solutions containing PO only (Zhao, 2005). K^+ may impede separation of the smectite layers similar to Ca^{2+} (de Bussetti & Ferreiro, 2004), resulting in less adsorption of PO on H shale.

Models with two parameters including the Langmuir model (Langmuir, 1918), the Freundlich model (Freundlich, 1906), the D-R model (Dubinin & Radushkevich, 1947), the Tempkin model

https://doi.org/10.1180/clm.2018.2 Published online by Cambridge University Press

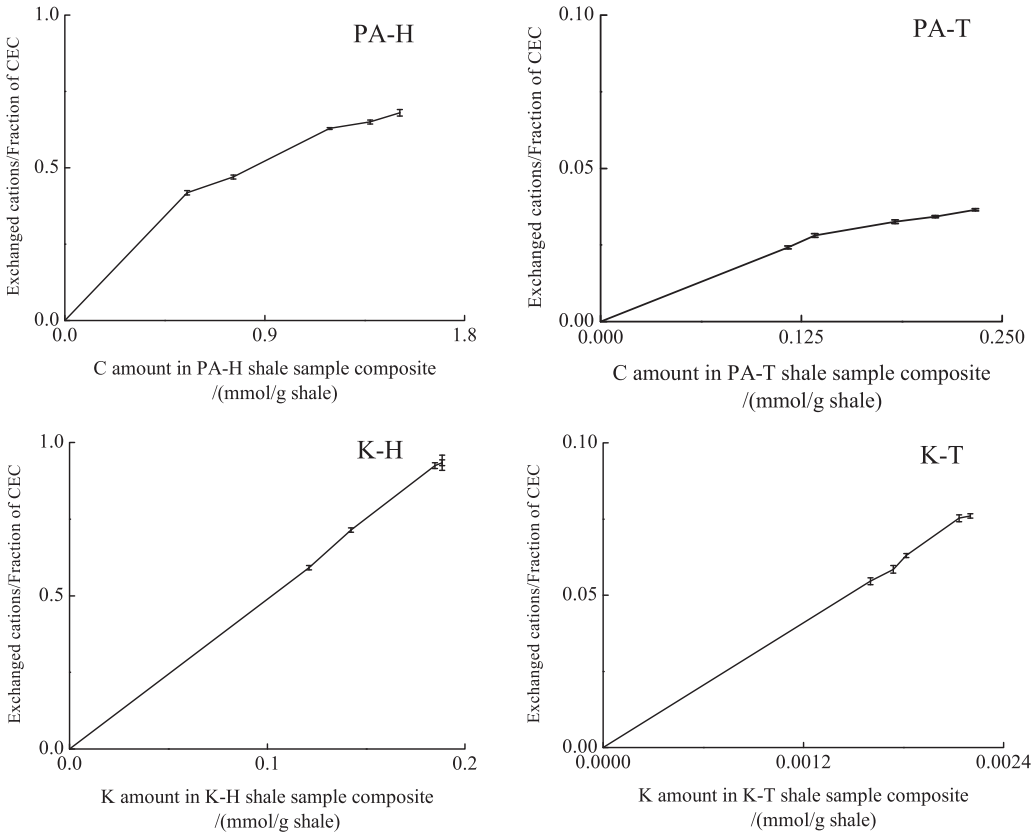

FIG. 2. The relationship between the released Na^+ content (normalized to CEC) and absorbed PA contents on H shale (PA-H) or T shale (PA-T); the relationship between the released Na^+ content (normalized to CEC) and absorbed PO content on H shale (K-H) or T shale (K-T). During PO adsorption on H or T shale, the released Na^+ content kept at zero; during PA adsorption on H or T shale in mixed solution of PA and KCl or PO adsorption on H or T shale in mixed solution of PO and KCl, the released Na+ content kept total Na^+ content in shale; during all adsorption processes, the released Ca_2^+, Mg_2^+ content kept at zero.

(Tempkin & Pyzhev, 1940), and those with three parameters including the Redlich-Peterson model (Redlich & Peterson, 1959), the Sips model (Sips, 1948), the Toth model (Toth, 1971), the Fritz-Schlunder model (Fritz & Schlunder, 1974) and the Khan model (Khan *et al.*, 1996), listed in Table 2, were used to fit the adsorption isotherms in Fig. 1. The adjusted R^2 coefficients were used as error functions and the fitting results are listed in Table 3. In Table 3 the best-fitting models with larger adjusted R^2 coefficient are shown with bold numbers. In the H-PO adsorption isotherms, the adjusted R^2 coefficients for all models were less than 0.980, indicating more heterogeneous adsorption sites for PO adsorption in the H shale. The highest R^2 coefficients (0.999), were observed for adsorption isotherms (H-K-PA, H-K-PO, T-K-PA, T-K-PO) in mixed solutions. It is inferred that adsorption on clay layers became the only adsorption mechanism for PA or PO in mixed solutions.

d_{001} spacings of smectite in shales and shale composites

The difference in d_{001}-spacing of smectite at 98% RH compared to that at ~0 RH resulted from intercalation of water, PA or PO molecules (Cases *et al.,* 1992, 1997; Zhao, 2010; Zhang *et al.,* 2016).

As shown in Fig. 3, in H shale, at ~0% RH, the smectite d_{001} spacing originally at 14.12 Å shifted to 14.21 Å after PA adsorption, to 14.24 Å after PO adsorption, to 13.95 Å after K^+ adsorption, to 13.97 Å

https://doi.org/10.1180/clm.2018.2 Published online by Cambridge University Press

TABLE 2. Equations describing the models used to model the adsorption isotherms in this study.

Models	Equation expression	Model constants	Constant constraints
	Two-parameter isotherms		
Freundlich	$Q^e = K_f C_e^{1/n}$	K_f, 1/n	n > 1
Langmuir	$Q^e = \frac{Q_m a_L C_e}{1 + a_L C_e}$	Q_m, a_L	–
D-R	$Q^e = Q_m exp\left(\frac{(RT\ln(1 + (1/C_e)))^2}{-2E^2}\right)$	Q_m, E	$Q_m > 0$, $E > 0$
Tempkin	$Q^e = \frac{RT}{b}\ln(K_{Te} C_e)$	K_{Te}, b	–
	Three-parameter isotherms		
Redlich-Peterson	$Q^e = \frac{K_R C_e}{1 + a_R C_e^{\beta}}$	K_R, a_R, β	$0 < \beta < 1$
Sips	$Q^e = \frac{Q_m b C_e^{1/n}}{1 + b C_e^{1/n}}$	Q_m, b, 1/n	$0 < 1/n < 1$
Toth	$Q^e = \frac{Q_m C_e}{(K_T + C_e^n)^{1/n}}$	Q_m, K_T, $1/n$	$0 < 1/n < 1$
Fritz-Schlunder	$Q^e = \frac{Q_m a_F C_e}{1 + Q_m C_e^n}$	Q_m, a_F, n	–
Khan	$Q^e = (Q_m b_K C_e)/(1 + b_K C_e)^{a_K}$	Q_m, b_K, a_K	–

* where; Q^e is equilibrium solid phase concentration (mg/g) and C_e is equilibrium liquid phase concentration (mg/L) in all isotherm models. In all models, the Q_m parameter is relevant to the adsorption capacity. In the Freundlich isotherm model, K_f and n are isotherm parameters characterizing the adsorption capacity and intensity, respectively. In the Langmuir equation, a_L is the Langmuir constant related to the energy of adsorption. In the D-R isotherm, E is energy of adsorption. In the Tempkin isotherm, K_{Te} is equilibrium binding constant (L/g), b is related to heat of adsorption (J/mol), R is the gas constant (8.314×10^{-3} kJ/K mol) and T is the absolute temperature (K). K_R (L/g) and a_R (L/mg) are Redlich–Peterson isotherm constants and β is the exponent which lies between 0 and 1. In the Sips isotherm, b is the constant related to energy of adsorption and 1/n is the model exponent. K_T, is the Toth model constant and n the Toth model exponent ($0 < n \leq 1$). a_F is the Fritz-Schlunder model constant and n is the Fritz-Schlunder model exponent. b_K is the Khan model constant and a_K is the Khan model exponent. Adjusted R^2 was used as the error function during isotherms fitting.

TABLE 3. Adjusted R^2 coefficients of adsorption isotherms with various models.

	H-PA	H-PO	T-PA	T-PO	H-K	T-K	H-K -PA	T-K -PA	H-K -PO	T-K -PO
Freundlich	**0.984**	0.960	**0.989**	0.899	0.982	**0.991**	0.881	0.996	0.913	0.975
Langmuir	0.968	**0.976**	0.946	0.958	0.969	0.970	0.978	0.998	0.967	0.996
D-R	0.812	0.926	0.848	0.994	0.949	0.955	0.985	0.994	0.991	0.997
Tempkin	0.976	0.969	0.977	0.938	**0.983**	0.988	0.923	0.997	0.943	0.981
Redlich-Peterson	0.980	0.975	0.986	0.990	0.977	0.988	0.998	0.998	0.994	**0.999**
Sips	0.981	0.975	0.985	0.998	0.979	0.988	0.997	**0.999**	0.996	0.998
Toth	0.981	0.975	0.985	**0.999**	0.978	0.988	**0.999**	0.998	**0.999**	0.998
Fritz-Schlunder	0.980	0.950	0.986	0.990	0.977	0.988	0.998	0.998	0.994	0.967
Khan	0.979	0.975	0.986	0.978	0.977	0.988	0.997	0.998	0.989	0.998

https://doi.org/10.1180/clm.2018.2 Published online by Cambridge University Press

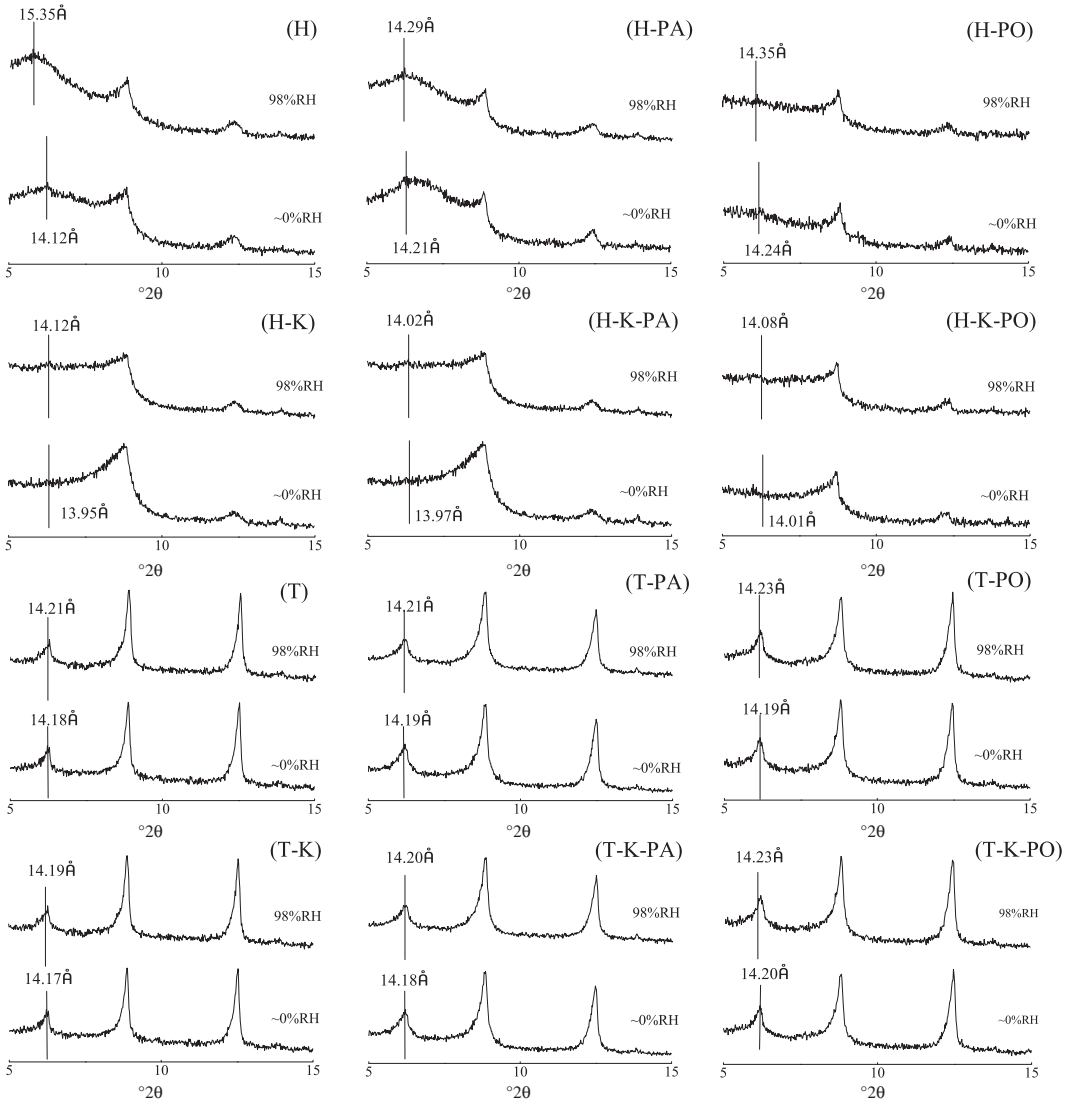

FIG. 3. XRD traces of shale and shale composites at p/p_o of ~0% RH or 98% RH (H or T, XRD trace of the H or T shale; H-PA or T-PA, XRD trace of the H or T shale with PA adsorption balanced; H-PO or T-PO, XRD trace of the H or T shale with PO adsorption balanced; H-K or T-K, d001-value test spectrum of the H shale or T shale with K^+ adsorption balanced; H-K-PA or T-K-PA, XRD trace of the H or T shale with PA adsorption balanced in mixed solution; H-K-PO or T-K-PO, XRD trace of the H or T shale with PO adsorption balanced in mixed solution).

after both K^+ and PA adsorption, and to 14.01 Å after adsorption of both K^+ and PO. Therefore, the d_{001} spacing of smectite increased after PA or PO adsorption, and decreased after adsorption of K^+ and K^+ along with PA, or PO. It is inferred that PA or PO may intercalate into clay layers of Na-smectite in H shale, while the intercalation may be prevented by K^+ adsorption.

At ~98% RH, the smectite d_{001} spacing increased by 1.23 Å in H shale, by 0.08 Å in H-PA shale composites, by 0.11 Å for H-PO shale composites, by 0.17 in H-K shale composites, by 0.05 in H-K-PA

https://doi.org/10.1180/clm.2018.2 Published online by Cambridge University Press

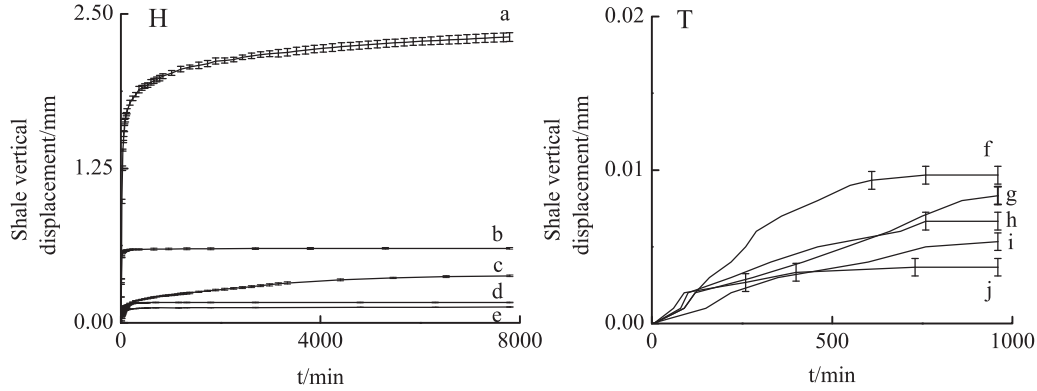

FIG. 4. Oedometer swelling tests of H shale immersed in 15 mmol/L PA solution (a), in 1 mol/L KCl solution (b), in 40 mmol/L PO solution (c), in mixed solution of 1 mol/L KCl and 40 mmol/L PO (d), in mixed solution of 1mol/L KCl and 15 mmol/L PA (e) and that of T shale immersed in 1 mol/L KCl solution (f), in 40 mmol/L PO solution (g), in 15 mmol/L PA solution (h), in mixed solution of 1 mol/L KCl and 40 mmol/L PO (i), in mixed solution of 1 mol/L KCl and 15 mmol/L PA (j).

shale composites, and by 0.07 for H-K-PO shale composites. K^+, PA and PO may reduce intercalation of water into clay layers and, when K^+ was used together with PA or PO, intercalation water was reduced further.

In the T shale, at ~0% RH, the d_{001} spacing of smectite was comparable after K^+, PA or PO adsorption. At ~98% RH, no obvious variation of d_{001} spacing was observed for T shale or T shale composites. It is inferred that in the T shale containing Ca-smectite, few water, PA or PO molecules intercalate into the clay layers.

Shale oedometer swelling tests and immersion tests in KCl, PA or PO solutions

Larger vertical swelling displacements of H shale were induced in all solutions compared to T shale (Fig. 4). The driving force for the hydration of the swelling clays (Na-smectite) is mainly hydration of Na^+ (Salles *et al.,* 2007), which causes greater hydration in the H shale which is richer in Na-smectite than the T shale. In H shale, the vertical displacements (2.303 mm) in 15 mmol/L PA solution were larger, with a large amount of micro fractures developing on the surface of H shale due to PA intercalation into smectite (Figs 3, 5).

In 1 mol/L KCl solution, vertical displacements were reduced to 0.590 mm with a few micro fractures on the surface of H shale (Fig. 5). Interactions between clay minerals and water include nonpolar or Lifshitz-van der Waals (LW) interactions and polar or acid-base (AB) interactions, specifically Lewis acid-base or electron-acceptor/electron-donor interactions (Van Oss *et al.,* 1988). According to Zhang *et al.* (2016) the electron-acceptor abilities of K-smectite are greatly reduced because of the lower hydration energy of K^+ compared to Na^+ (Jorgensen, 2002) and the d_{001} spacing of smectite at ~98% RH was greatly reduced in H shale (Fig. 3).

In 40 mmol/L PO solution, vertical displacement of H shale increased gradually to 0.341 mm in 5.4 days, with a few micro fractures on the surface (Fig. 5). PO adsorbed on the clay layer or coordinated with Na may reduce the water adsorption sites, while PO intercalation into smectite in H shale may also cause swelling displacement. As is shown in Fig. 5, after 2 h in KCl or PA solution, no dry area was observed on the shale surfaces, whereas in H shale in PO solution, part of the shale surface still remained dry even after 4 h. It is inferred that in PO solution, water-molecule transport was greatly reduced.

In the H shale, mixed solutions caused much less displacement (0.120 mm in KCl and PA solution, 0.164 mm in KCl and PO solution). After PA or PO adsorption, the H-bonding between water molecules and basal tetrahedral oxygens and the coordination between water molecules and exchangeable cations may be reduced (Zhang *et al.,* 2015, 2016). Hydration of Na^+ was greatly reduced when Na^+ was exchanged by K^+ due to the lower hydration energy of the latter. As a result, shale stability may improve in mixed solutions.

In the T shale, the vertical swelling displacements ranged from 0.04 to 0.11 mm without significant variation between the different solutions. Similar to the H shale, vertical displacement was lowest in KCl+PA solution (0.04 mm), and those of KCl+PO solution, PA solution, PO solution, KCl solution were 0.004, 0.005,

https://doi.org/10.1180/clm.2018.2 Published online by Cambridge University Press

0.006, 0.007 and 0.010, respectively (Fig. 4). Compared with Na-smectite, the divalent cations (Ca^{2+}) may impede separation of the smectite layers (de Bussetti & Ferreiro, 2004), causing less swelling due to hydration of T shale. With less Na^+ hydration, the H-bonding between water molecules and the oxygens of the siloxane surfaces of the clay contribute mostly to T shale hydration. K^+ may reduce hydration of Na^+ whereas PA or PO may reduce hydration of the clay layer. As a result, PA or PO inhibited swelling of T shale better.

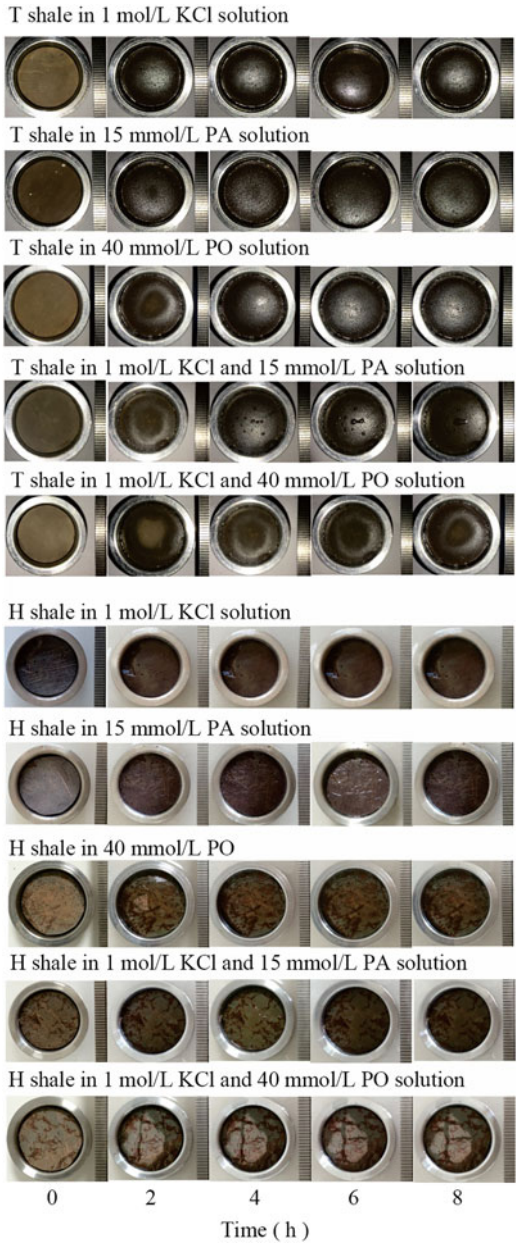

FIG. 5. Digital images of H or T shale before and after immersion in solutions.

CONCLUSIONS

In shale containing mainly Na-smectite, cation exchange and adsorption on the clay layer contributed to the adsorption of PA. Adsorption by H-bonding between PO and the clay layer and coordination between PO and exchange cations contributed to the adsorption of PO without ion exchange. Both PA and PO intercalated into Na-smectite, causing great swelling displacements, many fractures and instability of the shale. In mixed solutions (KCl+PA, KCl+PO), K^+ prevented PA or PO intercalation in smectite. PA or PO adsorption on shale reduced the H-bonding between water and clay layers and the coordination between water molecules and exchange cations. Meanwhile, K^+ replaced Na^+ reducing cation hydration. As a result, better stability of shale can be achieved in mixed solutions for shale containing mainly Na-smectite.

In shale containing mainly Ca-smectite, clay-layer adsorption was the main mechanism for adsorption of both PA and PO, and Ca^{2+} was not exchanged. No obvious differences in swelling displacement were observed for the various solutions. As a result, PA and PO should be used together with KCl during drilling in shale formations containing Na-smectites whereas in shales containing Ca-smectite any of PA, PO or KCl may be used alone.

ACKNOWLEDGMENT

The work presented in this paper is supported by CNPC under Award Number 2016ZX05020-003, 2016ZX05052-003, 2016E-0608.

REFERENCES

ASTM D 4546–96: Standard test methods for one-dimensional swell or settlement potential of cohesive soils. *Annual Book of ASTM Standards*, **04** (08). ASTM International, West Conshohocken, 1–7.

Burchill S., Hall P.L., Harrison R., Hayes M.H.B., Langford J.I., Livingston W.R., Smedley R.J., Ross D.K. & Tuck J. J. (1983) Smectite-polymer interactions in aqueous systems. *Clay Minerals*, **18**, 373–397.

De Bussetti S.G. & Ferreiro E.A. (2004) Adsorption of poly(vinyl alcohol) on montmorillonite. *Clays and Clay Minerals*, **52** (3), 334–340.

https://doi.org/10.1180/clm.2018.2 Published online by Cambridge University Press

Caenn R. & Chillingar G.V. (1996) Drilling fluids: state of the art. *Journal of Petroleum Science and Engineering*, **14**, 221–230.

Cases J.M., Bébrend I., Besson G., François M., Uriot J.P., Thomas F. & Poirier J.E. (1992) Mechanism of adsorption and desorption of water vapor by homoionic montmorillonite. 1. The sodium-exchanged form. *Langmuir*, **8**, 2730–2739.

Cases J.M., Bébrend I., François M., Uriot J.P., Michot L. J. & Thomas F. (1997) Mechanism of adsorption and desorption of water vapor by homoionic montmorillonite. 3. The Mg (super 2+), Ca (super 2 +), and Ba (super 3+) exchanged forms. *Clays and Clay Minerals*, **45** (1), 8–22.

Cui Y.N. & Van Jeroen S.D. (2010) Adsorption of polyetheramines on montmorillonite at high pH. *Langmuir*, **26**, 17210–17217.

Deng Y.N., Dixon J.B. & White G.N. (2006) Bonding mechanisms and conformation of poly(ethylene oxide)-based surfactants in interlayer of smectite. *Colloid and Polymer Science*, **4** (284), 347–356.

Dubinin M.M. & Radushkevich L.V. (1947) The equation of the characteristic curve of activated charcoal. *Proceedings of the Academy of Sciences, Physical Chemistry Section*, **55**, 331.

Freundlich H.M.F. (1906) Over the adsorption in solution. *Journal of Physical Chemistry*, **57**, 385–470.

Fritz W. & Schlunder E.U. (1974) Simultaneous adsorption equilibria of organic solutes in dilute aqueous solution on activated carbon. *Chemical Engineering Science*, **29**, 1279–1282.

Greenwell H.C., Harvey M.J., Boulet P., Bowden A.A., Coveney P.V. & Whiting A. (2005) Interlayer structure and bonding in nonswelling primary amine intercalated clays. *Macromolecules*, **38**, 6189–6200.

Heidug W. K. & Wong S.-W. (1996) Hydration swelling of water-absorbing rocks: a constitutive model. *International Journal for Numerical Analytical Methods in Geomechanics*, **20**, 403–430.

Jiang G.L. & Zhang P.P. (2005) Process and application of bentonite. Beijing, *Chemical Industry Press*, 44–48.

Jorgensen T.C. (2002) *Removal of ammonia from wastewater by ion exchange in the presence of organic compounds*. PhD research dissertation, Department of Chemical & Process Engineering, Canterbury University, New Zealand.

Khan A.R., Al-Waheab I.R. & Al-Haddad A. (1996) Generalized equation for adsorption isotherms for multicomponent organic pollutants in dilute aqueous solution. *Environmental Technology*, **17**, 13–23.

Langmuir I. (1918) The adsorption of gases on plane surfaces of glass, mica and platinum. *Journal of the American Chemical Society*, **40**, 1361–1403.

Mao H.J., Guo Y.T., Wang G.J. & Yang C.H. (2010) Evaluation of impact of clay mineral fabrics on hydration process. *Rock and Soil Mechanics*, **31**, 2722–2728.

Nelson A. & Cosgrove T. (2005) Small-angle neutron scattering study of adsorbed pluronic tri-block copolymers on laponite. *Langmuir*, **21**, 9176–9182.

Qu Y.Z., Lai X.Q., Zou L.F. & Su Y.N. (2009) Polyoxyalkyleneamine as shale inhibitor in water-based drilling fluids. *Applied Clay Science*, **44**, 265–268.

Redlich O.J. & Peterson D.L. (1959) A useful adsorption isotherm. *Journal of Physical Chemistry*, **63**, 1024–1026.

Rosa R.S., Rosa A., Farias S.B., Garcia M.H. & Coelho A. D.S. (2005) A new inhibitive water-based fluid: a completely cationic system. SPE 94523, *SPE Latin American and Caribbean Petroleum Engineering Conference*, 20–23 June, Rio de Janeiro, Brazil.

Salles F., Bildstein O., Douillard J.M., Jullien M. & Van Damme H. (2007) Determination of the driving force for the hydration of the swelling clays from computation of the hydration energy of the interlayer cations and the clay layer. *Journal of Physical Chemistry*, **111**, 13170–13176.

Sips R. (1948) On the structure of a catalyst surface. *Journal of Physical Chemistry*, **16**, 490–495.

Souza C.E.C.D., Lima A.S. & Nascimento R.S.V. (2010) Hydrophobically modified poly(ethyleneglycol) as reactive clays inhibitor additive in water-based drilling fluids. *Journal of Applied Polymer Science*, **117**, 857–864.

SY/T 5163, 1995. The relative amounts of sedimentary clay minerals X-ray diffraction analysis. *People's Republic of China Oil and Gas Industry Standards*, China Petroleum Industry Press, Beijing.

SY/T 5983, 1995. Identification of interlayered illite/smectite minerals by X-ray diffraction. *People's Republic of China Oil and Gas Industry Standards*, China Petroleum Industry Press, Beijing.

SY/T 6210, 1996. Quantitative analysis of total contents of clay minerals and common non-clay minerals in sedimentary rocks by x-ray diffraction. *People's Republic of China Oil and Gas Industry Standards*, China Petroleum Industry Press, Beijing.

Tempkin M.I. & Pyzhev V. (1940) Kinetics of ammonia synthesis on promoted iron catalysts. *Acta Physicochimica URSS*, **12**, 217–222.

Toth J. (1971) State equations of the solid gas interface layer. *Acta Chimica Hungarica*, **69**, 311–317.

Van Oss C.J., Chaudhury M.K. & Good R.J. (1988) Interfacial Lifshitz-van der Waals and polar interactions in macroscopic systems. *Chemical Reviews*, **88** (6), 927–941.

Wang L., Liu S.Y., Wang T. & Sun D.J. (2011) Effect of poly(oxypropylene) diamine adsorption on hydration and dispersion of montmorillonite particles in aqueous solution. *Colloids and Surfaces A*, **381**, 41–47.

Zhang S.F., Qiu Z.S. & Huang W.A. (2015) Water-adsorption properties of Xiazijie montmorillonite

https://doi.org/10.1180/clm.2018.2 Published online by Cambridge University Press

intercalated with polyamine. *Clay Minerals*, **50** (4), 537–548.

Zhang S.F., Sheng J.J. & Qiu Z.S. (2016) Water adsorption on kaolinite and illite after polyamine adsorption. *Journal of Petroleum Science and Engineering*, **142**, 13–20.

Zeynali M.E. (2012) Mechanical and physico-chemical aspects of wellbore stability during drilling operations. *Journal of Petroleum Science and Engineering*, **82–83**, 120–124.

Zhao Z.G. (2005) *Principles for Adsorption Application*. Chemical Industry Press, Beijing, pp. 184–194.

Zhong H.Y., Qiu Z.S., Huang W.A. & Cao J. (2011) Shale inhibitive properties of polyether diamine in water-based drilling fluid. *Journal of Petroleum Science and Engineering*, **78**, 510–515.

https://doi.org/10.1180/clm.2018.2 Published online by Cambridge University Press